HHS Public Access

Author manuscript

Nat Neurosci. Author manuscript; available in PMC 2015 December 01.

Published in final edited form as:

Nat Neurosci. 2015 June ; 18(6): 817–825. doi:10.1038/nn.4019.

Regulation of axon regeneration by the RNA repair/splicing pathway

Yuanquan Song[1], **David Sretavan**[2], **Ernesto A Salegio**[3], **Jim Berg**[1,4], **Xi Huang**[1], **Tong Cheng**[1], **Xin Xiong**[1], **Shan Meltzer**[1], **Chun Han**[1,5], **Trong-Tuong Nguyen**[2], **Jacqueline C. Bresnahan**[3], **Michael S. Beattie**[3], **Lily Yeh Jan**[1], and **Yuh Nung Jan**[1,*]

[1]Departments of Physiology and Biochemistry, University of California, San Francisco, Howard Hughes Medical Institute, San Francisco, CA 94158

[2]Departments of Ophthalmology and Physiology, University of California, San Francisco, San Francisco, CA 94143

[3]Brain and Spinal Injury Center, Department of Neurological Surgery, University of California, San Francisco, CA 94114

Abstract

Mechanisms governing a neuron's regenerative ability are important but not well understood. We identified Rtca, RNA 3′-terminal phosphate cyclase, as an inhibitor for axon regeneration. Removal of dRtca cell-autonomously enhanced axon regrowth in the *Drosophila* central nervous system, whereas its overexpression reduced axon regeneration in the periphery. Rtca along with the RNA ligase Rtcb and its catalyst Archease operate in the RNA repair/splicing pathway important for stress induced mRNA splicing, including that of Xbp1, a cellular stress sensor. dRtca and dArchease had opposing effects on Xbp1 splicing, and deficiency of dArchease or Xbp1 impeded axon regeneration in *Drosophila*. Moreover, overexpressing mammalian Rtca in cultured rodent neurons reduced axonal complexity *in vitro*, whereas reducing its function promoted retinal ganglion cell axon regeneration after optic nerve crush in mice. Our study thus links axon regeneration to cellular stress and RNA metabolism, revealing new potential therapeutic targets for treating nervous system trauma.

*Correspondence and requests for materials should be addressed to Y.N.J (yuhnung.jan@ucsf.edu).
[4]Present address: Allen Institute for Brain Science, Seattle, WA 98103
[5]Present address: Weill Institute for Cell and Molecular Biology, Department of Molecular Biology and Genetics, Cornell University, Ithaca, NY 14853

The authors declare no competing financial interests.

AUTHOR CONTRIBUTIONS

Y.S. carried out most of the experiments and performed the data analysis. D.S. performed the optic nerve crush experiment, E.A.S. performed LacZ staining, J.B. performed Rtca expression analysis, X.H. contributed to the neuronal culture experiment, T.C. contributed to the RGC axon regeneration analysis, X. X. performed the motor axon regeneration assay, S.M. contributed to the stress assay, C.H. made the *UAS-dRtca* fly strain, T.N. contributed to the optic nerve crush experiment, J.C.B. and M.S.B. contributed to the mouse axon regeneration experiment, Y.S., L.Y.J. and Y.N.J. together conceived the research and wrote the manuscript.

SUPPLEMENTARY INFORMATION

Online Methods

Supplementary Figures 1–15

Supplementary References (43–54)

INTRODUCTION

Failure of damaged axons to regenerate is the primary cause for permanent disabilities after central nervous system (CNS) injury and the non-reversible neurologic dysfunction in neurodegenerative diseases. The ability of a neuron to regenerate its axon after trauma is governed by the interaction between its intrinsic growth capacity and the local environment[1–4]. Notwithstanding the discoveries of extracellular factors and intrinsic pathways that reduce the regenerative capacity of axons[5–11], effective therapies have not yet emerged because removing the known inhibitory cues only partially restores regeneration, thus indicating the presence of additional inhibitory machineries that remain to be discovered.

Studies using model organisms such as *C. elegans* have begun to identify new genes important for axon regeneration[12, 13], illustrating the power of the genetic approach. To identify additional factors essential for controlling axon regeneration, we have recently established a *Drosophila* sensory neuron injury model that exhibits class specific axon regeneration, and demonstrated that the class IV dendritic arborization (da) neuron is capable of regenerating its axon in the periphery but exhibits limited regrowth inside the CNS, resembling its mammalian counterpart at the phenotypic and molecular levels[14]. Utilizing this model, we have performed a candidate-based genetic screen focusing on axotomy-regulated genes from multiple organisms[15–20] and identified *dRtca*/*CG4061* (RNA 3′-terminal phosphate cyclase), a cellular RNA processing enzyme with unknown biological function[21], as an inhibitor for CNS axon regeneration. Furthermore, we find that dArchease, a RNA ligase co-factor, functions downstream of dRtca as a pro-regeneration factor. Rtca and Archease are components of the RNA repair/splicing pathway, and regulate the nonconventional mRNA splicing of *Xbp1*, a stress sensor. Thus, *Xbp1* acts as a substrate, readout and downstream effector for the regulation of axon regeneration by the RNA repair/splicing pathway.

RESULTS

dRtca loss of function enhances axon regeneration

To assess axon regeneration, we used a previously described protocol[14]. Briefly, with a two-photon laser, we severed the axons of class IV da neurons (labeled with *ppk-CD4tdGFP*) within the ventral nerve cord (VNC) (Supplementary Fig. 1) of 2nd instar larvae (at 48 hours after egg laying, h AEL), confirmed the degeneration of the remaining axons after one day (at 72 h AEL) and assessed their regeneration after two more days (120 h AEL) (Fig. 1a–g). Compared to wild types (WT), which showed limited regrowth (Fig. 1a, arrows), new axons regrew from the retracted axon stems and extended into the commissure region, forming elaborate branches and reconnected commissure segments in a loss of function (LOF) allele of *dRtca* – *dRtca*^{NP5057} (Fig. 1b, arrowheads), an insertional allele with a P-element inserted in the 5′-UTR, disrupting mRNA splicing and reducing transcript expression (Supplementary Fig. 2a). Similar phenotypes were seen in trans-heterozygotes of *dRtca*^{NP5057} over a deficiency line *Df(1)BSC718* that lacks the *dRtca* locus (Fig. 1c), in a *dRtca* deletion allele *dRtca*$^{\Delta}$ generated from imprecise excision of *dRtca*^{NP5057} (Fig. 1d), and even stronger phenotypes were seen in *dRtca*$^{\Delta mat}$ in which both the zygotic and

maternal transcripts were removed (Fig. 1e). *dRtca*^{NP5057} is homozygous viable and fertile, so they were derived from homozygous mutant mothers. The mothers of *dRtca*^{NP5057}/ *Df(1)BSC718* trans-heterozygotes and *dRtca*$^{\Delta}$ mutants were heterozygous for *dRtca* and may provide maternal wild type *dRtca* transcripts. The fact that *dRtca*$^{\Delta mat}$ mutants, in which both the zygotic and maternal transcripts were removed, showed a stronger phenotype than *dRtca*$^{\Delta}$ zygotic mutants confirmed the maternal effect. Thus, the stronger phenotype of *dRtca*^{NP5057} mutants compared to *dRtca*^{NP5057}/ *Df(1)BSC718* trans-heterozygotes and *dRtca*$^{\Delta}$ mutants is likely because no wild type maternal transcripts were provided to *dRtca*^{NP5057} mutants. The function of *dRtca* is cell-autonomous because its RNAi knockdown in class IV da neurons (*ppk-Gal4>dRtcaRNAi*) (Fig. 1f, arrowheads) but not in glial cells (*repo-Gal4>dRtcaRNAi*) (Fig. 1g, arrows) recapitulated the enhancement of regeneration. The regeneration phenotype was further quantified by assessing the "Regeneration percentage", "Terminal branching" and "Commissure regrowth" (Fig. 1k, l, Supplementary Fig. 3a and Methods), as described previously[14]. The regenerating axons are illustrated in schematic diagrams with "Terminal branching" marked in red, "Commissure regrowth" in blue and other regrowing axons in black (Fig. 1a–g). The enhancement of regeneration is unlikely to be due to developmental defects of axon outgrowth because (1) The overall axon patterning of class IV da neurons in the uncut VNC is grossly normal (Supplementary Fig. 2b); (2) Reducing *dRtca* function in *dRtca*$^{\Delta}$ mutants or trans-heterozygotes of *dRtca*^{NP5057} over *Df(1)BSC718*, or via *dRtca* RNAi in class IV da neurons did not result in obvious defects of axon terminal patterning in the VNC (Supplementary Fig. 2c).

We next tested whether reducing *dRtca* function would trigger a regenerative response in neurons normally incapable of regeneration by severing their axons in *dRtca* mutants (Fig. 1h–j). Indeed, *dRtca* removal in class III da neurons (labeled with *19-12-Gal4>CD4tdGFP*, *repo-Gal80*), which unlike class IV da neurons did not regrow their axons that were severed in the periphery (Fig. 1h, arrow), elicited substantial regeneration in *dRtca*$^{\Delta mat}$ mutants (Fig. 1i, arrowheads) and after RNAi knockdown of *dRtca* specifically in class III da neurons (*19-12-Gal4>dRtcaRNAi*) (Fig. 1j, arrowheads), leading to a significant increase in the "Regeneration percentage", "Regeneration index" and "Regeneration length" (Fig. 1m–o, Supplementary Fig. 3b and Methods).

dRtca gain of function reduces axon regeneration

Conversely, overexpression of *dRtca* in class IV da neurons (*ppk-Gal4>dRtca*) mildly reduced their regenerative potential in the peripheral nervous system (PNS). In WT class IV da neurons, which regenerated about 74% of the time, new axons extended beyond the lesion site and followed along the axonal track (Fig. 2a, arrowheads). In contract, *dRtca* overexpression caused the incidence of regeneration to be reduced to 48% (Fig. 2b, arrow) and the length of the new axons to be significantly shortened as well (Fig. 2c–e). These data indicate that dRtca is an inhibitor of axon regeneration; not only does its removal cell-autonomously enhance axon regeneration in the CNS and enable regenerative incompetent neurons such as class III da neurons to regrow their axons in the PNS, its overexpression in regenerative competent neurons impedes axon regeneration in the periphery.

Furthermore, the inhibitory function of dRtca is not limited to sensory neurons, because *dRtca* overexpression in motor neurons also suppressed motor axon regeneration after nerve crush, as demonstrated by the reduced elaboration of growth cones (Fig. 3 and Methods).

The expression pattern of dRtca

We next examined the expression pattern of dRtca via two approaches. First, the P-element inserted in *dRtca* 5′-UTR (*dRtca*^{NP5057}) contains *Gal4*, which is in the same orientation as *dRtca*, thus can infer *dRtca* expression via a *UAS* reporter. We found that the *dRtca-Gal4>CD4tdGFP* reporter co-localized with the class IV da neuron marker *ppk-CD4tdTomato* (Fig. 4a), confirming its presence in class IV da neurons. Whereas *dRtca-Gal4* expression was observed in other tissues in the PNS and VNC (Fig. 4a, b), our analyses indicate that dRtca functions cell autonomously in neurons to inhibit axon regeneration.

Second, we generated a polyclonal antibody against dRtca and showed that the dRtca protein was present in WT but not in *dRtca*$^{\Delta mat}$ null class IV and class III da neurons, and was enriched in the nucleus (Fig. 4c, dashed circles). dRtca was also present in other types of multidendritic (md) neurons (Fig. 4c).

Interaction of dRtca with known regeneration regulators

To begin to understand the mechanisms underlying dRtca's role in regeneration, we first sought to determine how it genetically interacts with the known axon regeneration regulators: *Pten* and *Rac1*. Deletion of *Pten* (phosphatase and tensin homolog), a negative regulator of the mammalian target of rapamycin (mTOR) pathway, has been shown to increase CNS axon regeneration in both mammals and flies[8, 14, 22]. Overexpression of *dRtca* in the *Pten* mutant background (*Pten*^{MGH6}*; ppk-Gal4>dRtca*) or overexpression of *Pten* in *dRtca* null mutants (*dRtca*$^{\Delta}$*; ppk-Gal4>Pten*) largely abolished the enhancement of axon regeneration as seen in the VNC in *Pten*^{MGH6} or *dRtca*$^{\Delta}$ mutants (Fig. 5a, b). This suggests that *dRtca* and *Pten* likely function in parallel pathways. Interestingly, double mutants of *dRtca* and *Pten* (*dRtca*^{NP5057}*; Pten*^{MGH6}) did not further improve regeneration, as compared to *dRtca* mutants (Supplementary Fig. 4a, b), indicating the presence of additional brakes on regeneration. The regeneration phenotype in *dRtca* mutants appears to be comparable if not stronger than *Pten* mutants (*Pten*^{MGH6}, a hypomorphic allele) or *Akt* overexpression (*ppk-Gal4>Akt*) (Supplementary Fig. 4c, d).

Because the cytoskeleton regulator Rac GTPase is required for regenerative axon outgrowth in *C. elegans*[23], we overexpressed *Rac1* in class IV da neurons (*ppk-Gal4>Rac1*) and found an increase in the number of axons initiating the regenerative response in the VNC but not Terminal branching or Commissure regrowth, a partial improvement of regeneration (Fig. 5a–c, arrowheads). Conversely, overexpressing the dominant negative form of *Rac1* abolished the enhancement of CNS axon regeneration seen in *dRtca* null mutants (*dRtca*$^{\Delta mat}$*; ppk-Gal4>Rac1DN*) (Fig. 5a, b), whereas *Rac1DN* overexpression alone in class IV da neurons did not result in obvious axon regeneration defects in the PNS (Supplementary Fig. 4e–g). It thus seems likely that *Rac1* functions downstream of *dRtca* in a pathway that converges onto the regulation of the cytoskeleton.

RNA repair/splicing pathway regulates axon regeneration

Rtca is a RNA processing enzyme that possesses the RNA-3′-phosphate cyclase activity and catalyzes the ATP-dependent conversion of a 3′ phosphate to a 2′,3′-cyclic phosphodiester at the end of RNA[21]. The RNA 2′,3′-cyclic phosphate ends play important roles in RNA metabolism, for example, as intermediates during RNA repair by ligases[24, 25]. Rtcb (RNA 2′,3′-cyclic phosphate and 5′-OH ligase) represents a new type of RNA ligases that join 2′, 3′-cyclic phosphate and 5′-OH RNA ends to yield a 3′-5′ phosphodiester splice junction[24, 26–28]. Specifically, Rtcb is known to possess the cyclic phosphodiesterase activity, which hydrolyzes the 2′,3′-cyclic phosphate to a 3′-phosphate, as well as the ligase activity, which then joins the RNA 3′-phosphate to a 5′-OH RNA end. In addition, the specificity and efficacy of Rtcb's ligase activity can be enhanced by Archease[29, 30], which is a small acidic protein conserved in eukarya, bacteria and archaea[31]. In *E. coli*, RtcA and RtcB are encoded in a single operon, suggesting that they might cooperate to provide the healing and sealing function in a RNA repair pathway[27]. In one scenario, the healing refers to the restoration of ligatable 2′,3′-cyclic phosphate ends in the event that the inciting RNA damage directly generates RNA 3′-phosphates, or that the 2′,3′-cyclic phosphate products of RNA transesterification are further processed to a 3′-phosphate by a 2′,3′-cyclicphosphodiesterase[32]. However, this model cannot readily be reconciled by the subsequent finding that RtcB is adept at joining 3′-phosphate/5′-OH ends or 2′,3′-cyclic phosphate/5′-OH ends[33, 34]. Therefore, the exact interrelationship between RtcA and RtcB remains undetermined. Interestingly, the RtcBA operon in *E. coli* is regulated by the σ54 coactivator RtcR, suggesting that the RNA repair functions are induced in response to cellular stress[21]. Whereas the biological role of Rtca remains unknown, the enzyme is speculated to function in some aspects of cellular RNA processing[21]. Taking into account these findings and our observations that Rtca loss of function enhances axon regeneration, we hypothesized that the Rtca-Archease dependent RNA repair/splicing pathway regulates axon regeneration. Specifically, we speculated that axon injury triggers a type of cellular stress leading to RNA damage/splicing, producing RNA 3′-phosphates that need to be processed and rejoined by the Rtcb ligase, which is catalyzed by Archease. Because Rtca converts RNA 3′-phosphate to 2′,3′-cyclic phosphate, it can slow down the ligation process and impede regeneration. Consequently, silencing Rtca promotes axon regeneration (Supplementary Fig. 5). Following this rationale, we then investigated the role of Archease in axon regeneration.

To determine the role of the *Drosophila Archease* (*dArchease*/*CG6353*) in axon regeneration, we first examined class IV da neuron axon regeneration in the periphery. To maximize the phenotype, we modified our PNS axon injury protocol as described previously[14]: axotomy was induced at 72 h AEL, degeneration was confirmed at 96 h AEL and regeneration was assayed at 120 h AEL. Different from WT neurons, which exhibited substantial regrowth of their severed axons, axon regeneration was significantly impaired in the *dArchease* LOF mutant allele $dArchease^{PBc01013}$, which is an insertional allele with a P-element inserted into the 5′-UTR thereby disrupting its mRNA splicing and eliminating *dArchease* transcripts (Supplementary Fig. 6), as revealed by a significant drop of the "Regeneration percentage", "Regeneration index" and "Regeneration length" (Fig. 6a–c). This phenotype was confirmed in trans-heterozygotes of $dArchease^{PBc01013}$ over a

deficiency line *Df(3R)ED6076* or *Df(3R)BSC678* that lacks the *dArchease* locus (Fig. 6a–c). $dArchease^{PBc01013}$ mutants are larval lethal. $dArchease^{PBc01013}$ mutants and $dArchease^{PBc01013}$/*DfED6076*, $dArchease^{PBc01013}$/*DfBSC678* trans-heterozygotes showed a similar phenotype, suggesting that $dArchease^{PBc01013}$ mutants is likely an amorphic allele. The function of *dArchease* is required cell-autonomously as class IV da neuron specific knockdown of *dArchease* (*ppk-Gal4>dArcheaseRNAi*) but not glial cell RNAi (*repo-Gal4>dArcheaseRNAi*) was sufficient to phenocopy the regeneration failure (Fig. 6a–c). Moreover, loss of function of both *dRtca* and *dArchease* ($dRtca^{NP5057}$; $dArchease^{PBc01013}$) completely abolished the axon regeneration promoting effect in the VNC seen in $dRtca^{NP5057}$ mutants (Fig. 6d, e), producing many retracted or stalled axon stems (Fig. 6f, arrows). This epistasis analysis indicates that *dArchease* is a pro-regeneration factor downstream of *dRtca*, and they act in opposing ways to regulate axon regeneration (Supplementary Fig. 5).

Xbp1 is a substrate of dRtca/dArchease in regeneration

What might be the RNA substrates processed by this dRtca-dArchease dependent RNA repair/splicing pathway for the regulation of axon regeneration? We investigated the X-box binding protein 1 (Xbp1) as a candidate substrate for the following reasons: (1) Cellular stress such as ER stress triggers an adaptive intracellular signaling cascade known as the unfolded protein response (UPR)[35]. One main branch of the UPR is the activation of Ire1, which cleaves *Xbp1* pre-mRNA in the cytoplasm, converting the unspliced *Xbp1μ*, a putative transcriptional repressor, into the unconventionally spliced *Xbp1s*, by eliminating a 26-nucleotide intron (23 in flies) that changes the open reading frame of the 3rd exon, resulting in a new protein with transcriptional activity[36]. Xbp1s directly activates ER stress target genes to facilitate refolding and also degradation of misfolded proteins[35]. (2) The RNA ligase Rtcb and its cofactor Archease are involved in the non-conventional splicing induced by the UPR, and Archease is required for the splicing of the *Xbp1* mRNA[37]. (3) Loss of *xbp1* function in *C. elegans* results in severely reduced axon regeneration[13]. To determine the function of Xbp1 in axon regeneration in the PNS and CNS, we used a mutant allele of $Xbp1^{k13803}$, an allele with a P-element inserted into its 5′-UTR thus reducing transcripts[38], and showed that axon regeneration in the periphery was mildly reduced (Fig. 6a–c). This defect was stronger in trans-heterozygotes of $Xbp1^{k13803}$ over a deficiency line *Df(2R)BSC484* that lacks the *Xbp1* locus (Fig. 6a–c), suggesting that $Xbp1^{k13803}$ is likely a hypomorphic allele. Class IV da neuron specific (*ppk-Gal4>Xbp1RNAi*) but not glia specific (*repo-Gal4>Xbp1RNAi*) RNAi of *Xbp1* reproduced the impairment of regeneration (Fig. 6a–c), indicating it functions cell-autonomously. Moreover, double mutants of *dRtca* and *Xbp1* ($dRtca^{NP5057}$; $Xbp1^{k13803}$) dampened the enhancement of CNS axon regeneration seen in $dRtca^{NP5057}$ mutants (Fig. 6d, e), indicating that Xbp1 is indeed a pro-regeneration factor downstream of dRtca. Consistent with these lines of evidence, overexpression of the spliced form *Xbp1s* in class IV da neurons significantly enhanced axon regeneration in the VNC (Fig. 6d, e), and it also promoted axon regeneration in the periphery when overexpressed in class III da neurons (Supplementary Fig. 7, arrowheads). The observations that *dRtca Xbp1* double mutants did not completely eliminate the enhanced regeneration phenotype in *dRtca* mutants, and that *Xbp1s* overexpression led to milder enhancement of regeneration

compared to *dRtca* LOF, suggest that additional substrates contribute to regeneration regulation.

In order to directly assess the nonconventional splicing of *Xbp1* mRNA *in vivo*, we resorted to the heat-shock paradigm. Fly larvae of various genotypes underwent a 40°C heat-shock and the abundance of *Xbp1* splice variants was assessed using semi-quantitative RT-PCR. The ratio of *Xbp1s*/*Xbp1μ* was then quantified. Heat-shock induced the expression of the spliced form *Xbp1s*. In contrast to the enhanced expression of *Xbp1s* in *dRtca* mutants, *Xbp1s* level was greatly reduced in *dArchease* LOF mutants. Double mutants of *dRtca* and *dArchease* resembled *dArchease* mutants in the reduction of *Xbp1* splicing (Fig. 6g, h). Taken together, these data indicate that dRtca and dArchease in the RNA repair/splicing pathway negatively and positively regulate the stress induced *Xbp1* mRNA splicing, respectively, so that Xbp1 acts as a readout and effector for the regulation of axon regeneration (Supplementary Fig. 5).

Mammalian Rtca inhibits CNS axon regeneration

Having established the role of dRtca in axon regeneration in *Drosophila*, we went on to determine whether its function is evolutionarily conserved in mammals. We started by examining the expression pattern of the mammalian ortholog of dRtca *in vitro*. Antibodies raised against human RTCA recognized rodent Rtca in the cell bodies and processes of cultured hippocampal neurons (Fig. 7a). Moreover, the expression of *Rtca* transcripts in the DRG *in vivo* increased progressively throughout development, reaching the highest level in adults (Fig. 7b). Remarkably, using quantitative RT-PCR, we found that *Rtca* transcript level in the DRG was significantly reduced following lesion of the sciatic nerve peripherally, but not lesion of the central axon branch of DRG neurons with a spinal cord hemisection (Fig. 7c). Since the peripheral processes of DRG neurons are capable of regeneration, whereas their central axons that project into the spinal cord fail to regrow after injury[39], the selective suppression of Rtca following peripheral injury supports the hypothesis that the persisting expression of Rtca is inhibitory to axon regeneration in the CNS. Furthermore, in agreement with the overexpression phenotype in flies, overexpression of Rtca in cultured hippocampal neurons reduced axon complexity, and dramatically reduced proximal axonal branching (Fig. 7d, e) without affecting total axon length, indicative of the inhibitory function of Rtca.

We next asked if knocking out Rtca during development enhances axon regeneration of adult retinal ganglion cells (RGCs) *in vivo*. For this purpose, we generated a mutant allele with a LacZ cassette inserted after the 3rd exon (Supplementary Fig. 8a) to disrupt splicing and reduce transcription (reduced to ~19%, Supplementary Fig. 8b), thereby generating $Rtca^{LacZ\_loxP}$ ($Rtca^{Ins/Ins}$) mutant mice. Rtca protein level was also reduced to ~18% in the mutants (Supplementary Fig. 8c), suggesting this is likely a hypomorphic allele. Homozygous $Rtca^{Ins/Ins}$ mice were born, although fewer in number than expected from the mendelian ratio. By adulthood, there were no obvious differences in RGC number or RGC axon morphology among mutant ($Rtca^{Ins/Ins}$), het ($Rtca^{Ins/+}$) and WT ($Rtca^{+/+}$) animals (Supplementary Fig. 9a, c). Since the LacZ cassette is inserted into the *Rtca* locus, it can be used as a reporter for examining Rtca expression. LacZ staining was observed in the RGC

layer of *Rtca*$^{Ins/+}$ mice (Supplementary Fig. 10a–c) but not in *Rtca*$^{+/+}$ littermates (Supplementary Fig. 10d–f). Moreover, β-Galactosidase immunostaining in *Rtca*$^{Ins/+}$ mice showed distinct expression of the LacZ reporter within NeuN^{+} neurons in the retina, which was absent in *Rtca*$^{+/+}$ littermates (Supplementary Fig. 10g), indicating that Rtca is indeed expressed in RGCs. To assess RGC axon regeneration, we performed optic nerve crush in *Rtca*$^{Ins/Ins}$, *Rtca*$^{Ins/+}$ and *Rtca*$^{+/+}$ littermate mice at two developmental time points: postnatal day 35 (P35) and two–three months old, and the extent of axon regeneration was measured in the optic nerve after two weeks or three weeks, respectively. In mice injured at P35, compared to siblings (*Rtca*$^{Ins/+}$ and *Rtca*$^{+/+}$), which did not exhibit substantial axon regrowth beyond the crush site (Fig. 7f, asterisk indicates the crush site), *Rtca*$^{Ins/Ins}$ mutant mice showed a substantial increase in the number of regenerating axons at various distances from the injury site with some regenerating axons extending over 1.5 mm beyond the crush site (Fig. 7g, h). The regeneration enhancement in mice operated on at two-three months old was milder but still significant (Supplementary Fig. 11a–d). In these animals, curving, turning and looping of axons were observed, indicative of new axon growth (Supplementary Fig. 11b, arrowheads), and the furthest distance that axons travelled beyond the injury site was about 3.5 times longer in the mutants (Supplementary Fig. 11c). The crush site was further marked by the presence of ED1 staining, which labeled the infiltrating macrophages[40]. Whereas axons rarely penetrated beyond the ED1^{+} region in sibling controls, a large number of axons were seen hundreds of microns beyond the ED1^{+} region in *Rtca*$^{Ins/Ins}$ mutants (marked with asterisk in Supplementary Fig. 11e). Reducing Rtca function did not affect RGC survival after injury (Supplementary Fig. 9b), confirming that this increase in regenerating axons was not secondary to an increased RGC number. Our finding that reducing Rtca expression increased the regenerative potential of adult RGCs thus provides evidence for a potentially conserved role of Rtca as an anti-regeneration factor.

DISCUSSION

Our findings reveal an important role of the RNA repair/splicing pathway in regulating the intrinsic axon regeneration potential in response to PNS and CNS injury in *Drosophila*. Rtca and Archease integrate the injury signals triggered by axotomy and lead to the activation of downstream effectors such as the stress response cascade involving *Xbp1* splicing, and affect the ability of a neuron to regenerate. Axon injury has been suggested as a cellular stress and the mTOR pathway, a potential determinant of neuronal regeneration competence, could be inactivated under stress conditions such as hypoxia or DNA damage[41]. Interestingly, *Xbp1* splicing has been observed in RGCs after optic nerve injury and forced activation of Xbp1 promotes RGC survival[42]. Our work implicates that proper splicing of Xbp1 is also important for axon regeneration in *Drosophila*.

Moreover, recent work in *C. elegans* also suggests the involvement of stress response pathways, such as heat-shock, hypoxia and UPR, in axon regeneration[13]. However, how the injury signal is relayed to the stress response is unclear. Our work identifies a missing link and implicates the Rtca-Archease dependent RNA metabolism machinery as a regeneration regulator. *A priori*, axonal injury could either signal directly to the stress pathways, which then recruit Rtca-Archease, or alternatively, Rtca and Archease may represent injury

response elements upstream of the stress pathways. Our results showed that the Xbp1 dependent UPR pathway acts downstream of Rtca-Archease in controlling axon regeneration, and the remaining question is whether and how it impinges on other stress pathways, such as hypoxia or DNA damage. It will be important in future studies to identify other substrates in addition to Xbp1 that are modified by Rtca-Archease, and to search for response genes downstream of Xbp1. Our study raises the prospect of manipulating Rtca, Archease and Xbp1 as potential therapeutic interventions for treating nervous system injury.

As a first step to determine whether the Rtca pathway may have an evolutionarily conserved function in axon regeneration, we have examined CNS axon regeneration after optic nerve crush in a hypomorphic mouse mutant allele of Rtca and have suggestive evidence showing that may be indeed the case. The enhancement of RGC axon regeneration phenotype in the Rtca mutant is modest as compared to that seen in PTEN, KLF4 or SOCS3 knockouts. This may be due to the residual Rtca function in this hypomorphic allele or developmental compensation. Future experiments using mammalian injury models to examine the Rtca null allele, and to assess other components of the RNA repair/splicing pathway are therefore warranted to further define its potential role in axon regeneration.

METHODS

Fly stocks

ppk-CD4-tdGFP[43], *ppk-CD4-tdTomato*[43], *ppk-Gal4*[44], *repo-Gal4*[45], *19-12-Gal4*[46], *reop-Gal80*[47], *21-7-Gal4*[48], *hs-FLP; ppk-Gal4; UAS>CD2>mCD8-GFP*[49], *UAS-Pten* (Tian Xu lab), $Pten^{MGH6}$ (Iswar Hariharan lab) and *UAS-Xbp1s* (*UAS-Xbp1-RB*)[38] (Hyung Don Ryoo lab) have been previously described. *UAS-Dcr-2*, *Df(1)BSC718*, *Df(3R)Exel6186*, *Df(2R)BSC484*, *Dp(1;3)DC413*, *UAS-Rac1*, *UAS-Rac1DN*, $Xbp1^{k13803}$, *UAS-Xbp1RNAi*, *m12-Gal4*[50] ($P(Gal4)tey^{5053A}$) and *hs-FLPD5* were from Bloomington stock center. $dRtca^{NP5057}$ was from Kyoto DGRC. *UAS-dRtcaRNAi* and *UAS-dArcheaseRNAi* were from VDRC. $dArchease^{PBc01013}$ was from Exelixis. $dRtca^{\Delta}$ was generated from imprecise excision of $dRtca^{NP5057}$, in which the entire coding sequence of *dRtca* 3′ to the NP5057 insertion site together with the neighboring gene *CG4045* were replaced by a 3Kb fragment from the P element. To generate $dRtca^{\Delta mat}$, because $dRtca^{\Delta}$ males were sterile, a duplication stock *Dp(1;3)DC413*, which has a duplication of the region covering *dRtca* on the 3rd chromosome, was used. Specifically, $dRtca^{\Delta}$;; *Dp(1;3)DC413/TM6B* males were mated with $dRtca^{\Delta}$/*FM6* females to get the $dRtca^{\Delta}$ homozygous females. To generate the *UAS-dRtca* stock, the entire coding sequence of *dRtca* was cloned into the PUAST vector using the 5′-tgctccgattgttctgacac-3′ and 5′-attttccggcgcctttag-3′ primers. For experiments in *Drosophila*, both male and female larvae were used.

Mice

We used an embryonic stem (ES) cell from the European Conditional Mouse Mutagenesis Program (EUCOMM Project 82885) – a knockout-first line with a LacZ cassette inserted into the Rtca locus, to generate the Rtca mutant mouse (UCSF ES Cell Targeting Core). The resulting mouse $Rtca^{LacZ\_loxP}$ ($Rtca^{Ins/Ins}$) has a lacZ cassette inserted in-between the 3rd and 4th exons of *Rtca*, meanwhile, the 4th exon is flanked by loxP sites (Supplementary Fig.

8a). The lacZ insertion disrupted *Rtca* splicing and dramatically reduced transcript and protein levels (Supplementary Fig. 8b, c), and thus resulted in a hypomorphic allele. All mice were housed in an animal facility and maintained in a temperature-controlled and light-controlled environment with an alternating 12-hour light/dark cycle. Up to 5 mice of the same sex and similar age were housed in a cage. The animals had no prior history of drug administration, surgery or behavioral testing. All protocols have been approved by the UCSF Institutional Animal Care and Use Committee.

Sensory axon lesion in *Drosophila*

da neuron axon lesion and imaging in the PNS or within the VNC were performed in live fly larvae as previously described[14].

Quantitative analyses of sensory axon regeneration

Quantification was performed as previously described[14]. Briefly, for axon regeneration in the VNC, we used “Regeneration percentage”, which depicts the percent of regenerating commissure segments among all the segments that were severed; “Terminal branching”, which counts the number of axons that regenerated, reached the commissure bundle and appeared to form elaborate branches; “Commissure regrowth”, which counts the number of axons that had regenerated to connect the boundaries of commissure segments, longitudinally or laterally (Supplementary Fig. 3a). For axon regeneration in the PNS, we used “Regeneration percentage”, which depicts the percent of regenerating axons among all the axons that were lesioned; “Regeneration length”, which measures the increase of axon length; “Regeneration index”, which is calculated as an increase of “axon length”/“distance between the cell body and the axon converging point (DCAC)” (Supplementary Fig. 3b).

Live imaging

Live imaging was performed as described[51, 52]. Embryos were collected for 2 hours on yeasted grape juice agar plates and were aged at 25°C or room temperature. At the appropriate time, a single larvae was mounted in 90% glycerol under coverslips sealed with grease, imaged using a Leica SP5 microscope, and returned to grape juice agar plates between imaging sessions.

Generation of clones

FLP-out clones were produced as previously described[49].

Drosophila motor nerve crush assay and quantification

As described previously[53], the segmental nerves of 3rd instar larvae were pinched tightly through the cuticle for 5 s with Dumostar # 5 forceps, when the larvae were under CO_2 anesthesia. Larvae were then transferred to a grape plate and kept alive for varying periods of time at 25°C. For quantification of motor axon regeneration, the total area of the growth cone at 14.5 hours after crush was measured.

Neuronal cell culture, transfection and analysis

Hippocampal neurons were cultured from E19 Long-Evans rats at 150,000/ coverslip and maintained at serum-free B27-containing media. Plasmid transfections were done using Lipofectamine2000 (Invitrogen) at the indicated dates (div 0–3). For overexpression experiments, neurons were transfected with 0.75 μg of the Rtca expression construct (Open Biosystems) together with 0.5 μg GFP expressing plasmid (pLentilox 3.7). For axon analysis, we restricted all our morphological analysis to CTIP2 negative CA3 pyramidal neurons[54], and used Neurolucide (MBF Bioscience).

Optic nerve crush

For all *in vivo* experiments, optic nerve crush, tissue processing and imaging were performed in a double blind manner. P35 or 8–12 weeks old adult mice (male and female) were used, and the surgery was done by crushing the optic nerve behind the globe with forceps. The mice were then kept for 2 or 3 weeks respectively until perfusion. For the procedure performed at P35, RGC axons were anterogradely labeled through intravitreal injections of 1 μl cholera toxin subunit B (CtB555, 10μg/μl; Molecular Probes) two days before perfusion. Longitudinal sections (20 μm) were prepared and stained with anti-NF200 (labeling the neurofilament in axons) and anti-ED1 (labeling the infiltrating macrophages). The crush site was determined by the presence of ED1 staining, the clustering of NF200 staining, and/or the physical pinching/narrowing of the nerve. For quantification, the distance between the crush site and the tip of the longest axon was measured – Longest axon, and the number of axon fibers 50, 100, 150, 200, 250, 300, 350, 500, 750, 1000 and 1500 μm away from the crush site was counted for each section.

Quantification of RGC survival

Retina sections were immunostained with anti-Tuj1 (beta-III tubulin) to visualize RGCs and DAPI to detect nuclei. The number of RGCs were counted and normalized to the length of the corresponding retina region to calculate the RGC density. The RGC density from each sample was then normalized to the average value of the sibling controls.

Sciatic nerve lesion and spinal cord hemisection for expression analysis

For sciatic nerve lesion, mice were anesthetized (isoflurane) and the sciatic nerve was exposed at mid-thigh level, then sutured and transected distal to the ligature and the wound was closed. To lesion central processes of peripheral neurons, mice were anaesthetized (Ketamine (100 mg/kg)/ Xylazine (10 mg/kg)), then a laminectomy was performed at the thoracic level. The T6-T7 dorsal columns were then lesioned bilaterally using Dumont #5 Fine Forceps. In the cases of both peripheral and central nerve injury, L4 – L6 DRGs were collected 7 days after lesion for expression analysis. For each condition, DRGs from sham-operated mice (exposed but not lesioned sciatic nerve and thoracic laminectomy without dorsal column transaction) were used as controls.

Immunohistochemistry and LacZ staining

Immunohistochemistry analyses were performed on whole mount fly larvae, cultured neurons and on mouse tissue sections collected from OCT-embedded tissues. Primary

antibodies used were anti-Tuj1 (Covance, MMS-435P, 1:1,000), anti-Tau (Millipore, MAB3420, 1:1,000), anti-RTCA (Sigma, SAB2102059 and HPA027982, 1:200), anti-CTIP2 (Abcam, ab18465, 1:2,000), anti-NF200 (Sigma, N4142, 1:200), anti-ED1 (Abcam, ab31630, 1:200), anti-β-Galactosidase (MP Biomedicals cappel, 55976, 1:5,000) and anti-NeuN (Millipore, MAB377, 1:200). A custom-made antibody against the entire dRtca protein was generated (Thermo, 1:200). LacZ staining was performed using the Senescence β-Galactosidase Staining Kit (Cell signaling) according to manufacturer's instructions.

Heat-shock paradigm

In order to assess the stress induced splicing of *Xbp1*, 3rd instar larvae were heat-shocked at 40°C for 2 hours.

Quantitative RT-PCR

Semi-quantitative RT-PCR was done for *dRtca*, *α-tubulin*, *dArchease* and *Xbp1* in flies, and *Rtca* and *β-actin* in mice according to the manufacturer's protocols. The sequences were as follows: two regions of the *dRtca* transcripts were amplified with primers 5′-gaggaccaagctagcgattg-3′ and 5′-caagtaggagccgtcgatct-3′; 5′-caaacaggtctgcgttgatg -3′ and 5′-ctgtcatttgctcggctaca-3′. *α-tubulin* was amplified with 5′-acaacgaggctatctacgaca-3′ and 5′-ttttcagtgttgcagtgaattt-3′. Two regions of the *dArchease* transcripts were amplified with primers 5′-acactaagcggttgctggtt-3′ and 5′-ggtgatctccagcttcttgc-3′; 5′-cgagatttcctgccattgtt-3′ and 5′-gcaaaggggttgaaacagaa-3′. *Xbp1* was amplified with primers 5′-aggccatcaacgagtcactg-3′ and 5′-ctttccagagtgaggccagg-3′. Two regions of the mouse *Rtca* transcripts were amplified with primers 5′-tggatcatcacttggcaaaa-3′ and 5′-ggctagcgccatgaaaataa-3′; 5′-aacctttacccccgagaaga-3′ and 5′-aggacacagggcattgaaac-3′.

Real-time quantitative RT-PCR was done for mouse *Rtca*. 2μg of RNA was reverse transcribed to cDNA using iScript cDNA Synthesis Kit (Bio-Rad). All RNA concentrations were measured by NanoDrop 1000 Spectrophotometer. Real-time detection and quantification of cDNAs were performed with the iCycler instrument (Bio-Rad). Quantitative PCR was performed in a 20 μL reaction mixture using SYBR@GreenER qPCR Supermixes (Invitrogen). 50 cycles of amplification was performed according to manufacturer's instructions. Fluorescence data were collected at annealing stages and real-time analysis performed with iCycler™ iQ Optical System Software V3.0a. Serial dilutions of cDNAs were used for construction of the standard curve. Ct values were determined with automatically set baseline and manually adjusted fluorescence threshold. Gene expressions were normalized with that of *β-actin*.

Statistical analysis

No statistical methods were used to pre-determine sample sizes but our sample sizes are similar to those reported in previous publications[7–9, 14, 22] and the statistical analyses were done afterwards without interim data analysis. Data are expressed as mean ± SEM in bar and dot plots, or as median with min/max values in box-and-whisker plots. No data points were excluded. For the experiments done in *Drosophila*, data collection and analyses were not performed blind to the conditions of the experiments. For *in vivo* experiments in mice, optic nerve crush, tissue processing and imaging were performed in a double blind manner. Two-

tailed unpaired Student's t-test was performed for comparison between two groups of samples. One-way ANOVA followed by multiple comparison test was performed for comparisons among three or more groups of samples. Two-way ANOVA analyses were used to assess significance of multiple data points. Fisher's exact test was used to compare the percentage. The data meet the assumptions of the tests. The variance has been tested in each group of the data and the variance is similar among genotypes. Data distribution was assumed to be normal but this was not formally tested. The data were collected and processed randomly. Each experiment has been successfully reproduced at least three times and was performed on multiple days. Statistical significance was assigned, $*P < 0.05$, $**P < 0.01$, $***P < 0.001$.

A supplementary methods checklist is available.

Supplementary Material

Refer to Web version on PubMed Central for supplementary material.

Acknowledgments

We thank S. Younger, S. K. Ultanir, S. Yadav, D. Wang, S. Barbel, M. Tynan-La Fontaine and J. Sacramento for technical assistance; J. Martinez for advice on the Rtca pathway; I. Hariharan, T. Xu and H.D. Ryoo for fly lines; Bloomington Stock Center, Kyoto DGRC, VDRC and Exelixis for fly stocks; DGRC for plasmids; UCSF ES Cell Targeting Core for generating the knockout mouse; members of the Jan lab for helpful discussions. Y. S. is a recipient of the National Institute of Neurological Disorders and Stroke (NINDS) Pathway to Independence Award. This work was supported by a NINDS K99/R00 award (1K99NS088211-01) to Y.S., a National Science Foundation Graduate Research Fellowship (1144247) to S.M., a UC Irvine-Roman Reed Spinal Cord Injury grant (P0045665) to Y.N.J., a NIH grant (2R37NS040929) to Y.N.J., a NIH grant (EY010688-19) to D.S. and a Research to Prevent Blindness grant to D.S.. L.Y.J. and Y.N.J. are investigators of Howard Hughes Medical Institute.

References

1. Filbin MT. Recapitulate development to promote axonal regeneration: good or bad approach? Philos Trans R Soc Lond B Biol Sci. 2006; 361:1565–1574. [PubMed: 16939975]
2. Fitch MT, Silver J. CNS injury, glial scars, and inflammation: Inhibitory extracellular matrices and regeneration failure. Exp Neurol. 2008; 209:294–301. [PubMed: 17617407]
3. Goldberg JL, Klassen MP, Hua Y, Barres BA. Amacrine-signaled loss of intrinsic axon growth ability by retinal ganglion cells. Science. 2002; 296:1860–1864. [PubMed: 12052959]
4. Schwab ME, Bartholdi D. Degeneration and regeneration of axons in the lesioned spinal cord. Physiol Rev. 1996; 76:319–370. [PubMed: 8618960]
5. Case LC, Tessier-Lavigne M. Regeneration of the adult central nervous system. Curr Biol. 2005; 15:R749–753. [PubMed: 16169471]
6. Harel NY, Strittmatter SM. Can regenerating axons recapitulate developmental guidance during recovery from spinal cord injury? Nat Rev Neurosci. 2006; 7:603–616. [PubMed: 16858389]
7. Moore DL, et al. KLF family members regulate intrinsic axon regeneration ability. Science. 2009; 326:298–301. [PubMed: 19815778]
8. Park KK, et al. Promoting axon regeneration in the adult CNS by modulation of the PTEN/mTOR pathway. Science. 2008; 322:963–966. [PubMed: 18988856]
9. Smith PD, et al. SOCS3 deletion promotes optic nerve regeneration in vivo. Neuron. 2009; 64:617–623. [PubMed: 20005819]
10. Sun F, He Z. Neuronal intrinsic barriers for axon regeneration in the adult CNS. Curr Opin Neurobiol. 2010; 20:510–518. [PubMed: 20418094]
11. Yiu G, He Z. Glial inhibition of CNS axon regeneration. Nat Rev Neurosci. 2006; 7:617–627. [PubMed: 16858390]

12. Chen L, et al. Axon regeneration pathways identified by systematic genetic screening in C. elegans. Neuron. 2011; 71:1043–1057. [PubMed: 21943602]
13. Nix P, et al. Axon regeneration genes identified by RNAi screening in C. elegans. J Neurosci. 2014; 34:629–645. [PubMed: 24403161]
14. Song Y, et al. Regeneration of Drosophila sensory neuron axons and dendrites is regulated by the Akt pathway involving Pten and microRNA bantam. Genes Dev. 2012; 26:1612–1625. [PubMed: 22759636]
15. Bonilla IE, Tanabe K, Strittmatter SM. Small proline-rich repeat protein 1A is expressed by axotomized neurons and promotes axonal outgrowth. J Neurosci. 2002; 22:1303–1315. [PubMed: 11850458]
16. Costigan M, et al. Replicate high-density rat genome oligonucleotide microarrays reveal hundreds of regulated genes in the dorsal root ganglion after peripheral nerve injury. BMC Neurosci. 2002; 3:16. [PubMed: 12401135]
17. Fischer D, Petkova V, Thanos S, Benowitz LI. Switching mature retinal ganglion cells to a robust growth state in vivo: gene expression and synergy with RhoA inactivation. J Neurosci. 2004; 24:8726–8740. [PubMed: 15470139]
18. Nilsson A, Moller K, Dahlin L, Lundborg G, Kanje M. Early changes in gene expression in the dorsal root ganglia after transection of the sciatic nerve; effects of amphiregulin and PAI-1 on regeneration. Brain Res Mol Brain Res. 2005; 136:65–74. [PubMed: 15893588]
19. Veldman MB, Bemben MA, Thompson RC, Goldman D. Gene expression analysis of zebrafish retinal ganglion cells during optic nerve regeneration identifies KLF6a and KLF7a as important regulators of axon regeneration. Dev Biol. 2007; 312:596–612. [PubMed: 17949705]
20. Araki T, Milbrandt J. Ninjurin, a novel adhesion molecule, is induced by nerve injury and promotes axonal growth. Neuron. 1996; 17:353–361. [PubMed: 8780658]
21. Genschik P, Billy E, Swianiewicz M, Filipowicz W. The human RNA 3′-terminal phosphate cyclase is a member of a new family of proteins conserved in Eucarya, Bacteria and Archaea. EMBO J. 1997; 16:2955–2967. [PubMed: 9184239]
22. Liu K, et al. PTEN deletion enhances the regenerative ability of adult corticospinal neurons. Nat Neurosci. 2010; 13:1075–1081. [PubMed: 20694004]
23. Gabel CV, Antoine F, Chuang CF, Samuel AD, Chang C. Distinct cellular and molecular mechanisms mediate initial axon development and adult-stage axon regeneration in C. elegans. Development. 2008; 135:1129–1136. [PubMed: 18296652]
24. Popow J, et al. HSPC117 is the essential subunit of a human tRNA splicing ligase complex. Science. 2011; 331:760–764. [PubMed: 21311021]
25. Remus BS, Shuman S. A kinetic framework for tRNA ligase and enforcement of a 2′-phosphate requirement for ligation highlights the design logic of an RNA repair machine. RNA. 2013; 19:659–669. [PubMed: 23515942]
26. Englert M, Sheppard K, Aslanian A, Yates JR 3rd, Soll D. Archaeal 3′-phosphate RNA splicing ligase characterization identifies the missing component in tRNA maturation. Proc Natl Acad Sci U S A. 2011; 108:1290–1295. [PubMed: 21209330]
27. Tanaka N, Shuman S. RtcB is the RNA ligase component of an Escherichia coli RNA repair operon. J Biol Chem. 2011; 286:7727–7731. [PubMed: 21224389]
28. Tanaka N, Meineke B, Shuman S. RtcB, a novel RNA ligase, can catalyze tRNA splicing and HAC1 mRNA splicing in vivo. J Biol Chem. 2011; 286:30253–30257. [PubMed: 21757685]
29. Desai KK, Cheng CL, Bingman CA, Phillips GN Jr, Raines RT. A tRNA splicing operon: Archease endows RtcB with dual GTP/ATP cofactor specificity and accelerates RNA ligation. Nucleic Acids Res. 2014; 42:3931–3942. [PubMed: 24435797]
30. Popow J, Jurkin J, Schleiffer A, Martinez J. Analysis of orthologous groups reveals archease and DDX1 as tRNA splicing factors. Nature. 2014; 511:104–107. [PubMed: 24870230]
31. Canaves JM. Predicted role for the archease protein family based on structural and sequence analysis of TM1083 and MTH1598, two proteins structurally characterized through structural genomics efforts. Proteins. 2004; 56:19–27. [PubMed: 15162483]

32. Das U, Shuman S. 2′-Phosphate cyclase activity of RtcA: a potential rationale for the operon organization of RtcA with an RNA repair ligase RtcB in Escherichia coli and other bacterial taxa. RNA. 2013; 19:1355–1362. [PubMed: 23945037]
33. Tanaka N, Chakravarty AK, Maughan B, Shuman S. Novel mechanism of RNA repair by RtcB via sequential 2′,3′-cyclic phosphodiesterase and 3′-Phosphate/5′-hydroxyl ligation reactions. J Biol Chem. 2011; 286:43134–43143. [PubMed: 22045815]
34. Chakravarty AK, Shuman S. The sequential 2′,3′-cyclic phosphodiesterase and 3′-phosphate/5′-OH ligation steps of the RtcB RNA splicing pathway are GTP-dependent. Nucleic Acids Res. 2012; 40:8558–8567. [PubMed: 22730297]
35. Ron D, Walter P. Signal integration in the endoplasmic reticulum unfolded protein response. Nat Rev Mol Cell Biol. 2007; 8:519–529. [PubMed: 17565364]
36. Yoshida H, Matsui T, Yamamoto A, Okada T, Mori K. XBP1 mRNA is induced by ATF6 and spliced by IRE1 in response to ER stress to produce a highly active transcription factor. Cell. 2001; 107:881–891. [PubMed: 11779464]
37. Jurkin J, et al. The mammalian tRNA ligase complex mediates splicing of XBP1 mRNA and controls antibody secretion in plasma cells. EMBO J. 2014; 33:2922–2936. [PubMed: 25378478]
38. Ryoo HD, Domingos PM, Kang MJ, Steller H. Unfolded protein response in a Drosophila model for retinal degeneration. EMBO J. 2007; 26:242–252. [PubMed: 17170705]
39. Ramon y Cajal, S. Degeneration and Regeneration of the Nervous System. Oxford University Press; London: 1928.
40. Liu X, Hawkes E, Ishimaru T, Tran T, Sretavan DW. EphB3: an endogenous mediator of adult axonal plasticity and regrowth after CNS injury. J Neurosci. 2006; 26:3087–3101. [PubMed: 16554460]
41. Lu Y, Belin S, He Z. Signaling regulations of neuronal regenerative ability. Curr Opin Neurobiol. 2014; 27C:135–142. [PubMed: 24727245]
42. Hu Y, et al. Differential effects of unfolded protein response pathways on axon injury-induced death of retinal ganglion cells. Neuron. 2012; 73:445–452. [PubMed: 22325198]
43. Han C, Jan LY, Jan YN. Enhancer-driven membrane markers for analysis of nonautonomous mechanisms reveal neuron-glia interactions in Drosophila. Proc Natl Acad Sci U S A. 2011; 108:9673–9678. [PubMed: 21606367]
44. Grueber WB, Jan LY, Jan YN. Different levels of the homeodomain protein cut regulate distinct dendrite branching patterns of Drosophila multidendritic neurons. Cell. 2003; 112:805–818. [PubMed: 12654247]
45. Sepp KJ, Schulte J, Auld VJ. Peripheral glia direct axon guidance across the CNS/PNS transition zone. Dev Biol. 2001; 238:47–63. [PubMed: 11783993]
46. Xiang Y, et al. Light-avoidance-mediating photoreceptors tile the Drosophila larval body wall. Nature. 2010; 468:921–926. [PubMed: 21068723]
47. Awasaki T, Lai SL, Ito K, Lee T. Organization and postembryonic development of glial cells in the adult central brain of Drosophila. J Neurosci. 2008; 28:13742–13753. [PubMed: 19091965]
48. Song W, Onishi M, Jan LY, Jan YN. Peripheral multidendritic sensory neurons are necessary for rhythmic locomotion behavior in Drosophila larvae. Proc Natl Acad Sci U S A. 2007; 104:5199–5204. [PubMed: 17360325]
49. Grueber WB, et al. Projections of Drosophila multidendritic neurons in the central nervous system: links with peripheral dendrite morphology. Development. 2007; 134:55–64. [PubMed: 17164414]
50. Ritzenthaler S, Suzuki E, Chiba A. Postsynaptic filopodia in muscle cells interact with innervating motoneuron axons. Nat Neurosci. 2000; 3:1012–1017. [PubMed: 11017174]
51. Emoto K, Parrish JZ, Jan LY, Jan YN. The tumour suppressor Hippo acts with the NDR kinases in dendritic tiling and maintenance. Nature. 2006; 443:210–213. [PubMed: 16906135]
52. Parrish JZ, Emoto K, Kim MD, Jan YN. Mechanisms that regulate establishment, maintenance, and remodeling of dendritic fields. Annu Rev Neurosci. 2007; 30:399–423. [PubMed: 17378766]
53. Xiong X, et al. Protein turnover of the Wallenda/DLK kinase regulates a retrograde response to axonal injury. J Cell Biol. 2010; 191:211–223. [PubMed: 20921142]

54. Ultanir SK, et al. Chemical genetic identification of NDR1/2 kinase substrates AAK1 and Rabin8 Uncovers their roles in dendrite arborization and spine development. Neuron. 2012; 73:1127–1142. [PubMed: 22445341]

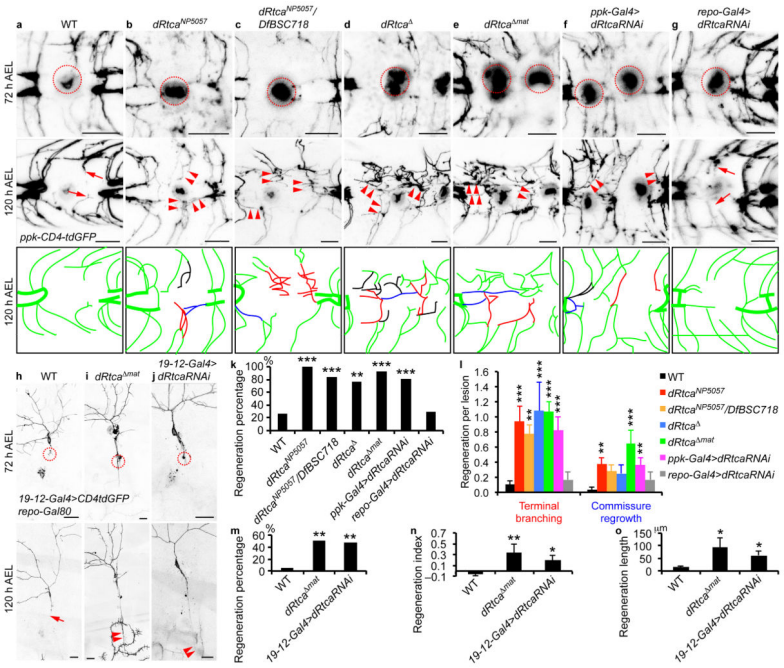

Figure 1. *dRtca* loss of function enhances axon regeneration in the CNS and PNS

(a–g) *dRtca* removal increases class IV da neuron axon regrowth in the VNC. The injury site is demarcated by the dashed circle. Limited regrowth is seen in WT (**a**, arrows). Increased regeneration is shown in *dRtca* LOF mutants (**b**, arrowheads), *dRtca* mutant over deficiency (**c**), *dRtca* zygotic deletion (**d**), *dRtca* zygotic and maternal deletion (**e**), class IV specific *dRtca* RNAi (**f**), but not in glia RNAi (**g**, arrows). The regenerating axons are illustrated in schematic diagrams with “Terminal branching” marked in red, “Commissure regrowth” in blue and other regrowing axons in black. **(h–j)** *dRtca* removal promotes class III da neuron axon regeneration in the periphery. Dashed circle marks the lesion site. Whereas WT class III da neurons fail to regenerate their axon in the PNS (**h**, arrow), *dRtca* zygotic and maternal deletion (**i**), and class III specific *dRtca* RNAi (**j**) elicit substantial regrowth (arrowheads). **(k)** *dRtca* LOF increases Regeneration percentage of class IV da neuron axons in the VNC (N = 46, 16, 18, 13, 14, 14, 14 lesioned segments for each genotype; $^{**}P < 0.01$, $^{***}P < 0.001$, Fisher’s exact test, $P < 0.0001$, $P < 0.0001$, $P = 0.0022$, $P < 0.0001$, $P < 0.0001$, $P = 1$). **(l)** *dRtca* LOF increases Terminal branching and Commissure regrowth in the VNC (N = 29, 8, 9, 6, 7, 11, 6 larvae for each genotype; $^{**}P < 0.01$, $^{***}P < 0.001$, one-way ANOVA followed by Dunnett’s multiple comparisons test). **(m–o)** *dRtca* LOF increases the Regeneration percentage ($^{**}P < 0.01$, Fisher’s exact test, $P = 0.0026$, $P = 0.0061$), Regeneration index ($^{*}P < 0.05$, $^{**}P < 0.01$, one-way ANOVA followed by Dunnett’s multiple comparisons test) and Regeneration length ($^{*}P < 0.05$, one-way ANOVA followed by Holm-Sidak’s multiple comparisons test; N = 19, 10, 17 neurons for each genotype) of class III da neuron axons in the PNS. Scale bar = 20 μm.

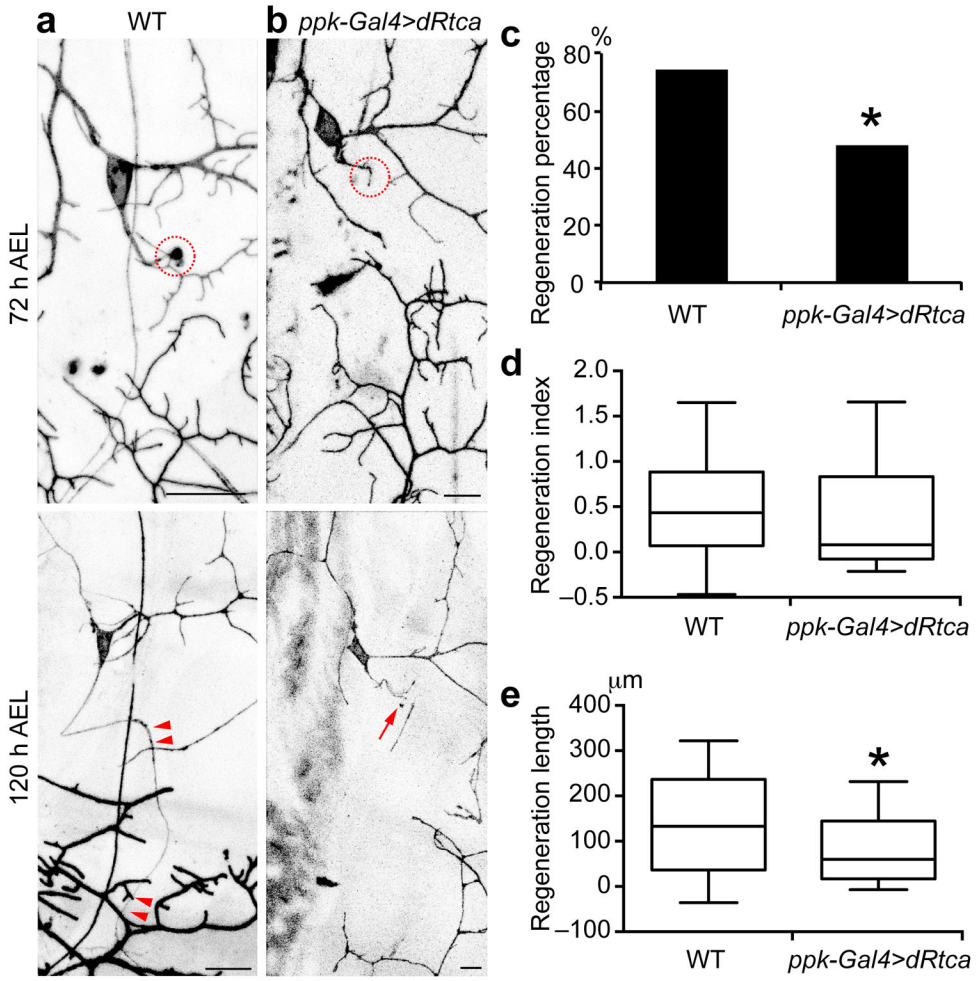

Figure 2. *dRtca* overexpression reduces axon regeneration in the PNS

(a) WT class IV da neurons show robust axon regrowth in the periphery (arrowheads, dashed circle marks lesion site). **(b)** *dRtca* overexpression in class IV da neurons mildly reduces their regeneration potential (arrow). **(c–e)** *dRtca* overexpression reduces the Regeneration percentage (*$P < 0.05$, Fisher's exact test, $P = 0.0398$) and Regeneration length (*$P < 0.05$, two-tailed unpaired Student's t-test, $P = 0.0458$; $N = 43$, 27 neurons for each genotype) of class IV da neuron axons in the PNS. Scale bar = 20 μm.

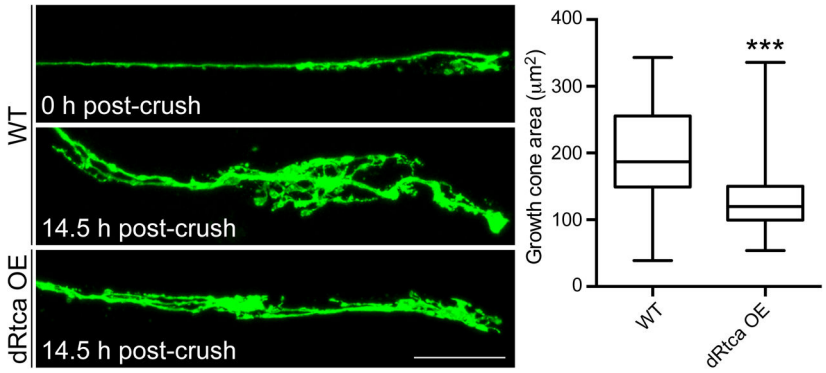

Figure 3. *dRtca* overexpression reduces motor axon regeneration

Right after crush, the growth cones of the segmental motor nerves (labeled by *m12-Gal4>CD4tdGFP*) display a simple morphology with very few filopodia. 14.5 hours after crush, motor axons in WT larvae regenerates substantially with elaborated growth cones. *dRtca* overexpression reduces their regeneration. The total area of the growth cones at 14.5 hours post-crush is measured, and it is significantly reduced by *dRtca* overexpression (N = 34, 33 nerves; ***$P < 0.001$, two-tailed unpaired Student's t-test). Scale bar = 20 μm.

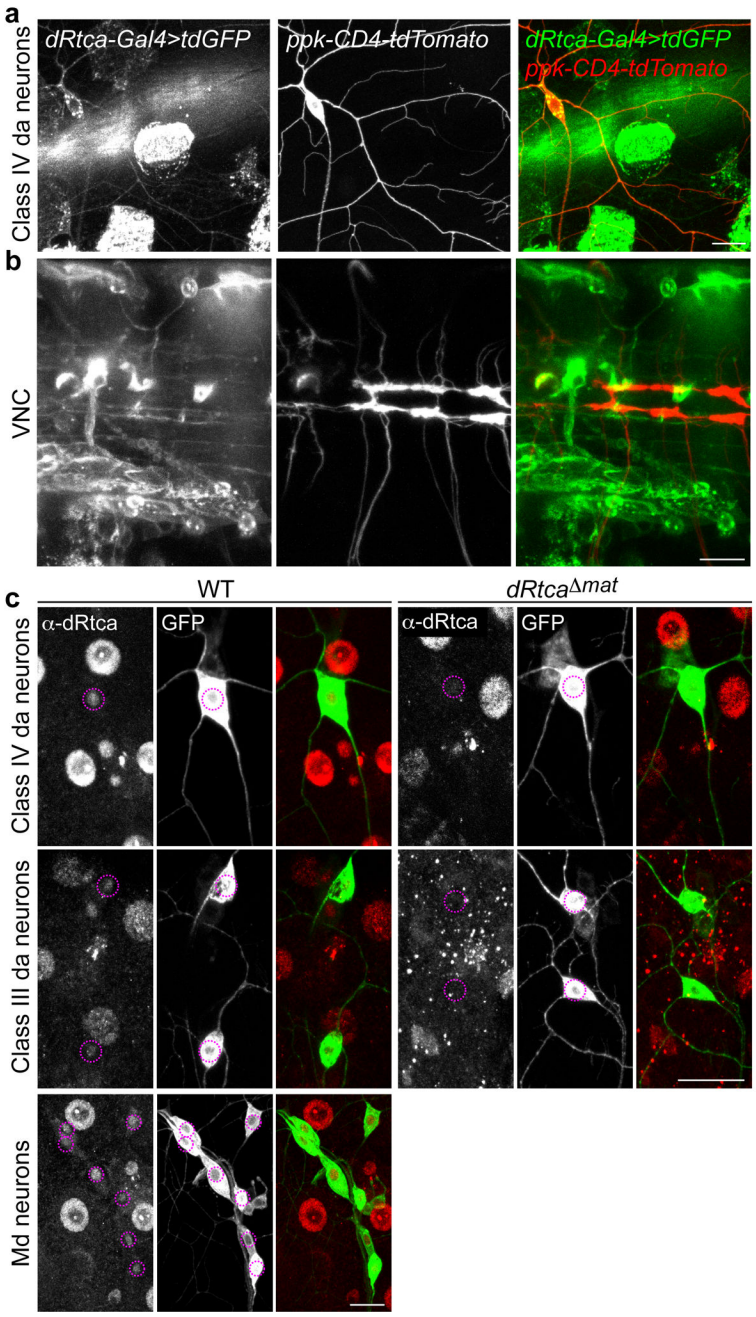

Figure 4. The expression pattern of dRtca in *Drosphila*

(a) The P-element inserted in *dRtca* 5'-UTR (*dRtca*^{NP5057}) contains *Gal4*, which is in the same orientation as *dRtca*, thus can infer *dRtca* expression via a *UAS* reporter. *dRtca-Gal4>CD4tdGFP* reporter co-localizes with the class IV da neuron marker *ppk-CD4tdTomato*, confirming its presence in class IV da neurons. **(b)** *dRtca-Gal4>CD4tdGFP* shows *dRtca* is expressed in other tissues within the VNC. **(c)** dRtca immunostaining shows that dRtca protein is present in class IV (labeled with *ppk-CD4tdGFP*) and class III (labeled with *19-12-Gal4>CD4tdGFP, repo-Gal80*) da neurons in WTs but not in *dRtca*$^{\Delta mat}$ nulls, enriched in the nucleus. dRtca is also present in other types of multidendritic (md) neurons

(labeled with *21-7-Gal4>CD4tdGFP*). Dashed circles mark the nucleus of da neurons. The big patch-like staining is present in both WT and $dRtca^{\Delta mat}$ nulls, and is likely nonspecific. Scale bar = 20 μm.

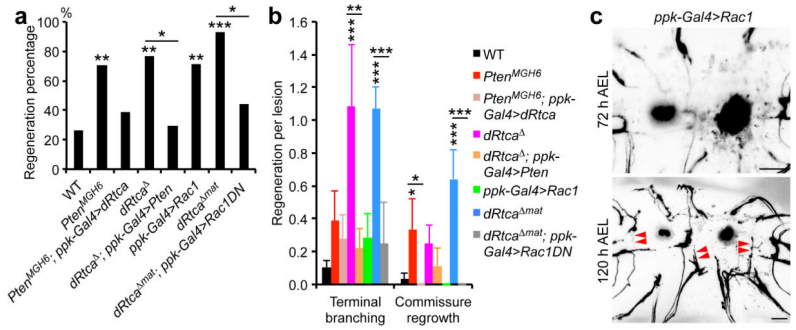

Figure 5. The interaction of dRtca with known regeneration regulators

(a–c) dRtca likely functions in parallel with the Pten pathway, Rac1 mildly promotes CNS axon regeneration and functions downstream of dRtca. Overexpression of *dRtca* in *Pten* mutants or overexpression of *Pten* in *dRtca* nulls largely abolishes the enhancement of axon regeneration in the VNC in $Pten^{MGH6}$ or $dRtca^{\Delta}$ mutants, as reflected by Regeneration percentage (**a**), Terminal branching and Commissure regrowth (**b**). Overexpression of *Rac1* in class IV da neurons increases the Regeneration percentage (**a**) without promoting Terminal branching or Commissure regrowth (**b**, **c**, arrowheads). Overexpressing the dominant negative *Rac1* abolished the enhancement of CNS axon regeneration seen in *dRtca* nulls (**a**, **b**) (*N*= 46, 17, 18, 13, 17, 14, 14, 9 lesioned segments in **a**; *N* = 29, 9, 9, 6, 9, 7, 7, 4 larvae in **b**, **P* < 0.05, ***P* < 0.01, ****P* < 0.001, Fisher's exact test in **a**, *P* = 0.0027, *P* = 0.3681, *P* = 0.0022, *P* = 0.7609, *P* = 0.0253, *P* = 0.0037, *P* < 0.0001, *P* = 0.4224, *P* = 0.0183; one-way ANOVA followed by Tukey's or Dunnett's multiple comparisons test in **b**). Scale bar = 20 μm.

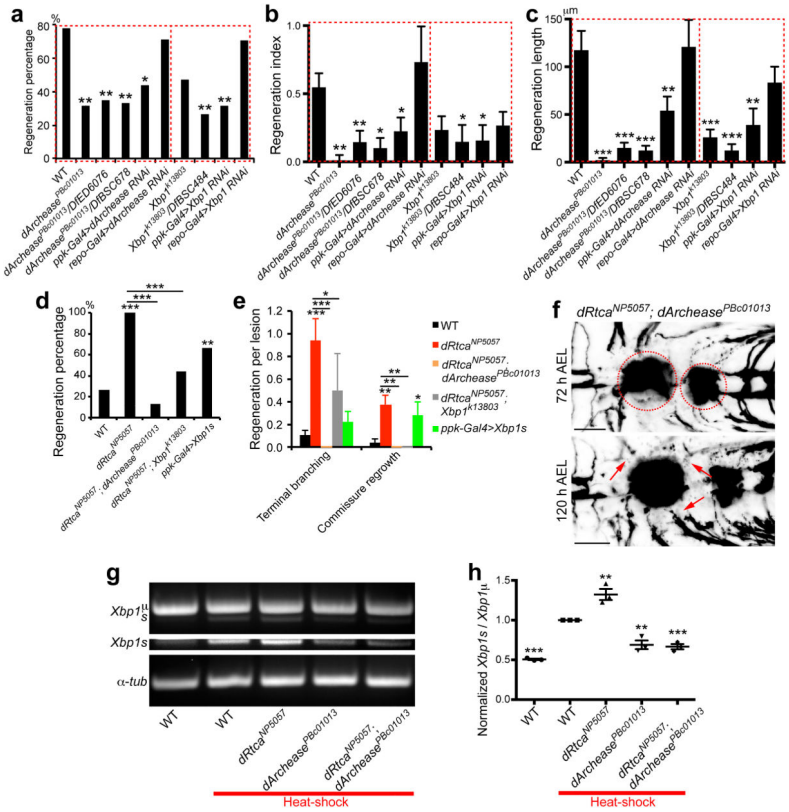

Figure 6. The dRtca pathway in regulating axon regeneration

(a–c) *dArchease* and *Xbp1* are required for class IV da neuron axon regeneration in the PNS. *dArchease* or *Xbp1* deficiency, shown in LOF mutants, mutant over deficiency, class IV da neuron specific RNAi, but not glia RNAi, impedes class IV da neuron axon regeneration in the periphery, as quantified by Regeneration percentage (**a**), Regeneration index (**b**) and Regeneration length (**c**) (*N*= 26, 16, 26, 18, 25, 20, 18, 15, 16, 17 neurons). **(d–f)** Epistasis analysis of *dRtca*, *dArchease* and *Xbp1* indicates that *dArchease* and *Xbp1* function downstream of *dRtca*. Double mutants of *dRtca* and *dArchease* completely diminish the enhancement of CNS axon regeneration in *dRtca* single mutants, while double mutants of *dRtca* and *Xbp1* show a milder attenuation. A representative image of the stalled axon regeneration in the VNC of *dRtca* and *dArchease* double mutants is shown in (**f**) (*N* = 46, 16, 15, 16, 18 lesioned segments in **d**; *N* = 29, 8, 7, 8, 9 larvae in **e**). **(g, h)** Heat-shock induces the splicing of the active form of *Xbp1* (*Xbp1s*), which is enhanced by *dRtca* LOF, but inhibited in *dArchease* LOF mutants, and double mutants of *dRtca* and *dArchease* (**g**). Blots were cropped and full-length images are presented in Supplementary Figure 12. The ratio of *Xbp1s*/*Xbp1μ* is quantified in (**h**) (*N* = 3 experiments; **P* < 0.05, ***P* < 0.01, ****P* < 0.001, Fisher's exact test in **a**, **d**, *P* = 0.004, *P* = 0.0023, *P* = 0.0049, *P* = 0.0217, *P* = 0.7406, *P* = 0.0581, *P* = 0.0025, *P* = 0.004, *P* = 0.7244 in **a**, *P* = 0.0001, *P* = 0.4831, *P* = 0.2178, *P* < 0.0001, *P* = 0.0008, *P* = 0.004 in **d**; one-way ANOVA followed by Dunnett's, Tukey's, Holm-Sidak's or Dunn's multiple comparisons test in **b**, **c**, **e**, **h**). Scale bar = 20 μm.

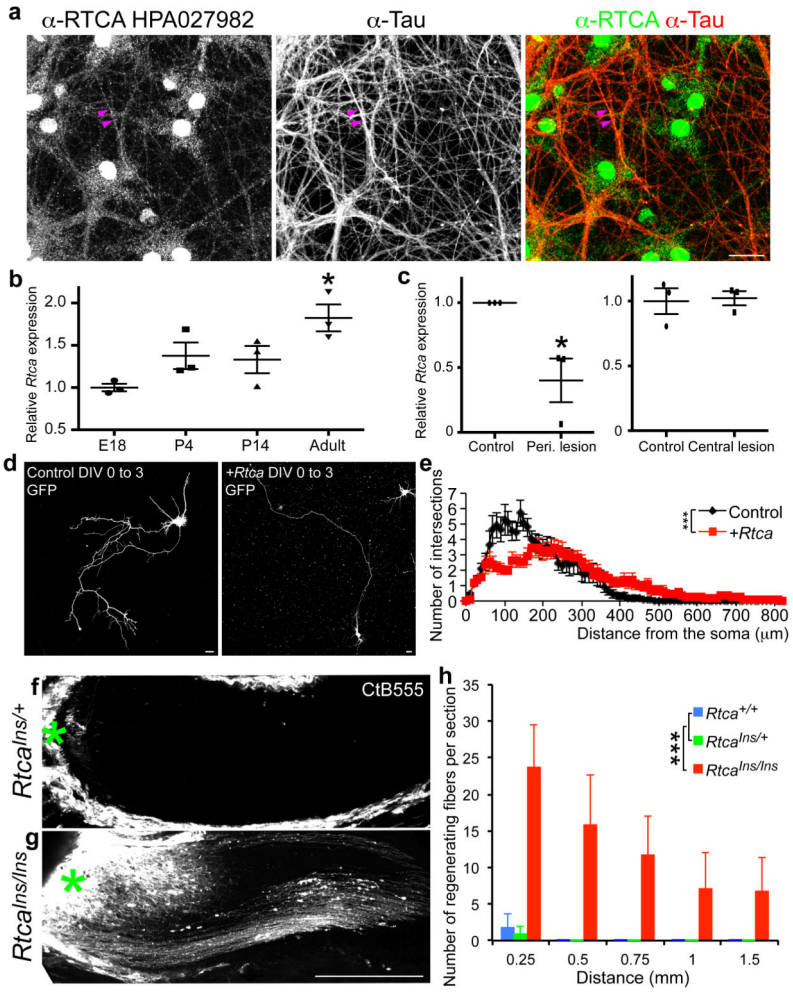

Figure 7. Rtca is an inhibitory factor for axon growth *in vitro* and RGC regeneration *in vivo* in rodents

(a) A RTCA antibody (HPA027982) recognizes endogenous Rtca in cultured hippocampal neurons. Rtca is present in the soma and neuronal processes (arrowheads), which are labeled with anti-Tau staining. Scale bar = 20 μm. **(b)** The expression of *Rtca* transcripts in the whole DRGs *in vivo* is upregulated throughout development, with the highest level in adults. (N = 3 experiments; the expression level of each data point was normalized to the average value of E18; *P < 0.05, one-way ANOVA followed by Dunnett's multiple comparisons test). **(c)** *Rtca* transcript level in the DRG is significantly reduced after a peripheral sciatic nerve lesion, whereas lesioning the central axon branch of DRG neurons with a spinal cord hemisection does not alter its expression (N = 3 experiments; for peripheral lesion, expression level of the lesioned DRG is normalized to the corresponding control DRG in pairs; for central lesion, expression level of each data point was normalized to the average value of Control; *P < 0.05, two-tailed unpaired Student's t-test, P = 0.0237, P = 0.8544). **(d**, **e)** Ectopic expression of Rtca in cultured hippocampal neurons reduces axon complexity when transfected from div (days *in vitro*) 0 to div 3, and dramatically reduces proximal axonal branching (N = 18, 18 neurons; ***P < 0.001, two-way ANOVA). Scale bar = 20 μm. **(f–h)** Two weeks after optic nerve crush in P35 adult siblings ($Rtca^{+/+}$ and $Rtca^{Ins/+}$),

and *Rtca*$^{Ins/Ins}$ mutant mice, regenerating fibers were labeled by intravitreal injection of Alexa 555-labeled cholera toxin B (CtB555). **(f**, **g)** Tissue sections through the optic nerve from a *Rtca*$^{Ins/Ins}$ mutant mice show regenerating axons more than 800 μm distal to the lesion site, whereas no obvious axon regrowth beyond the crush site is seen in similar sections from a sibling control (*Rtca*$^{Ins/+}$, asterisk marks the crush site). **(h)** Regenerating fibers were counted at specified distances from the lesion site. More fibers regenerate in *Rtca*$^{Ins/Ins}$ mice compared to siblings (N = 5 *Rtca*$^{+/+}$, 5 *Rtca*$^{Ins/+}$ and 6 *Rtca*$^{Ins/Ins}$ mice; ***P < 0.001, two-way ANOVA). Scale bar = 200 μm.